Title: 20,000 Leagues into the Cheese: An exploration of spatial organization in cheese rinds

Author:
Aspen T. Reese
Departments of Biology and of Molecular Genetics and Microbiology, Duke University
Box 90338, Biology Department Duke University, Durham, NC 27708.
aspen.reese@duke.edu

Abstract

Cheese rinds contain a diverse microbial community of fungi and bacteria. It is unknown how these communities vary with distance from the rind and whether this variation correlates with environmental variation within the rind. Such variation is predicted based on our knowledge of environmental sediment samples. To test whether it exists in cheese, oxygen and pH profiles were measured with microelectrodes. Community composition of bacterial and fungi was queried using FISH and chitin staining. A clear oxygen profile was observed and there is preliminary evidence of compositional variation. Future efforts to study cheese rind communities should take into account spatial variation in abiotic and biotic variables.

Introduction

Cheese rind communities have been proposed as a model system for studying microbial community assembly processes (Wolfe *et al*. 2014). These communities exhibit reproducible succession across the globe and can be experimentally tractable in the lab. They are home to an array of bacterial and fungal species that vary between cheeses with environmental conditions (most notably moisture and NaCl concentration). These microbes are predicted to interact within the cheese based on in vitro assays. And, as is the case in most microbial systems studied to date, these interactions can be mutualistic, commensal, or competitive (de Boer *et al*. 2005; Wargo and Hogan 2006; Bonfante and Anca 2009).

To date, research has sampled the rind as a whole (e.g. Feurer *et al*. 2004; Quigley *et al*. 2012; Wolfe *et al*. 2014). However, both physics (e.g. diffusion rates) and biology (e.g. metabolism) would lead us to predict that the environment within the rind should vary with distance from the edge. In particular, we would expect oxygen to be depleted with increasing distance from the rind edge as is seen in sediments (e.g. Revsbech *et al*. 1980). This abiotic variation would then be expected to cause variation in microbial community composition.

In this project, we set out to identify if there are profiles of abiotic conditions in cheese rinds and whether any variation in abiotic conditions correlate with differences in community composition. Abiotic variation from the rind into the curd was quantified using a Unisense microelectrode setup. Fluorescence in situ hybridization (FISH) was used on cryoembedded samples to identify microbial community variation and the spatial relationships between microbes throughout the cheese rinds. Three types of cheese were profiled.

Methods

Cheese Samples

Three types of cheese were studied for this report. All were produced by Jasper Hill Farm in Greensboro Vermont.

Moses Sleeper is a bloomy rind cheese. It is a brie type cheese which is associated with halotlerant, marine-associated Proteobacteria and the fungus *Penicillium camemberti*, which is added to the milk by the cheese makers.

Bayley Hazen Blue (hereafter referred to as Blue) is a natural rind cheese made from whole raw milk. It has spores of *Penicillium roqueforti* added to the milk, and the cheese makers purposefully introduce small holes in the cheese to aerate the cheese and increase growth of the *P. roqueforti*.

Willoughby is a washed rind cheese. This cheese is associated with yeast, Actinobacteria, and Proteobacteria. The production process limits the growth of filamentous fungi. (R. Dutton *pers. comm.*)

Microelectrode Profiles

Three different types of microsensors were used throughout this experiment: O_2 microsensors with a tip diameter of either 50 or 500um, a pH microelectrode with needle diameter of 1.1mm, and a temperature sensor with a diameter of 500um. The O_2 microsensors are amperometric and were connected to a picoampere amplifier in a multimeter (Unisense, Denmark). The pH microelectrode was connected to a high-impedance multivoltmeter input in the same multimeter. The temperature sensor was connected to the temperature channel in the same multimeter. Experimental setup and calibrations were following Cowley *et al*. (2015).

The O_2 sensors were Clark-type electrodes that respond linearly to changes in oxygen concentration. A two-point calibration was performed. An oxygen-free solution of 0.1M sodium hydroxide and 0.1M sodium ascorbate was used for the zero-oxygen reading and a 100% air-saturated 0.64% salt solution, was used for 288.554uM/L oxygen. The pH electrode has a detection limit of 0.1 pH unit and was calibrated with buffers of pH 4, 7, and 10. The temperature probe has a detection limit of 0.1°C and was calibrated at 0°C in ice milliQ water and 100°C in boiling milliQ water.

Microsensors were mounted on a motorized micromanipulator in a custom-made probe holder, allowing both the O2 and pH sensors to be used simultaneously. The reference electrode for pH and the temperature sensor were not used for depth profiling and instead were mounted separately with a stationary free-standing ring stand.

The sensors were positioned at the air-rind interface by visual inspection. Automatic profiling and data acquisition were conducted using SensorTrace Pro 2.3 software. The vertical profiles were measured in 50um steps to at least 2000um deep beginning at 500um above the surface. At each depth, the measuring time was 3seconds with 1 second between measuring points. At least three profiles were taken for each cheese. Profiles were conducted on at least two separate cheese samples on at least two separate days.

[Methodological notes: The Moses Sleeper proved particularly difficult to profile. For 5 of the 8 profiles taken (data not shown), the sensors did not enter the cheese cleanly but instead depressed the rind by pressing the curd outwards. This phenomenon resulted in high oxygen readings throughout the profile and therefore the data were not included in the analysis. Attempting to profile the cheese either while cold (just out of the 4°C) or at room temperature did not seem to affect the likelihood of this behavior. In the future, it might be worth trying to sample in a container that has walls that contain the cheese to prevent the oozing outward behavior.]

FISH

Cryoembedding

525mm^3 cubes of cheese were freshly cut and then placed into embedding molds atop a small amount of OCT. The cuts were then covered completely with OCT and stored overnight at 4°C. The following day, the molds were held in -20°C liquid ethanol (made by covering 0.75lbs dry ice with ethanol in a ice bucket) until they were completely frozen and opaque. Then the embedded product was separated from the mold and stored at -80°C until sectioning.

Cryosectioning

Sections of cryoembedded cheese were prepared using a Microm HM505NCryostat at the MBL Central Microscopy Facility. Embedded products were acclimated to the -24°C environment and then frozen to mounts using OCT. Following cutting, slices were picked up directly onto a microscope slide and allowed to melt on at room temperature. Sections ranging in size from 20um to 50um were prepared. All results presented were produced using 20um sections except for the confocal imaging which was done on 50um sections. Sections were taken from approximately 0, 100, 250, 500, 750, 1000um from the top of the rind. At least 3 sections of unique cheese pieces from each depth were taken and subjected to FISH.

[Methodological notes: 10um sections are also possible on the cryostat but consistently rolled before they could be picked up by the slide. 20um sections were the smallest size that could be reliably produced and picked up. For a single plane of analysis, however, a smaller section size would be better.]

Fixation

Immediately following sectioning, the samples were fixed in 4% PFA for 30minutes. The PFA was washed with excess PBS and then hybridized (mono-FISH) or permeablized (CARD-FISH). Fixation was preformed following sectioning on the recommendation of David Berry and Orest Kuzyk (University of Vienna) due to the high lipid content of the cheese samples, which would be solubilized if the samples were fixed before sectioning.

Permeablization.

For CARD-FISH, permeablization is necessary before hybridization to ensure that the probes will be properly taken up by the cells. Samples were permeablized using fresh lysozyme and chitinase solution (see Appendix for recipes). Slides were incubated in lysozyme for 30 minutes at 37°C in the dark and then washed in excess milliQ water. Then slides were incubated in chitinase for 20 minutes at 25°C (Baschien et al. 2001) and then washed in excess milliQ.

[Methodological notes: Chitinase permeablization was not fully successful because calcofluor (chitin stain) was able to stain treated sections. Future work should optimize chitin permeablization to reduce autofluorescence of fungi for CARD-FISH.]

Inactivation of Endogenous Peroxidases

For CARD-FISH, inactivation of endogenous peroxidases is necessary before hybridization to prevent activation of the probes before the probe is added. The samples were inactivated by incubating in a solution of 0.01M HCl containing 3% H2O2 for 15minutes at room temperature and then washed in excess milliQ and then 95% ethanol.

Hybridization

CARD hybridization buffer was prepared with 35% formamide (CARD buffer was used for both CARD-FISH and mono-FISH; see Appendix for recipe). 50ul 100:1 hybridization:probe mixture was applied to each section and spread to ensure even coverage. Each slide was then placed horizontally inside a 50ml falcon tube and a kimwipe soaked with 1ml of hybridization

buffer was added below the slide. These tubes were then incubated horizontally in the dark at 46°C for 150 minutes. The probes used included EUB338 I-III, EUK516, and NON338. Immediately following the hybridization, the slides were washed in washing buffer (see Appendix for recipe) for 10 minutes at 48°C and then in 1xPBS for 15 minutes at room temperature.

CARD-FISH Amplification

Amplification buffer from freezer stocks was used (see Appendix for recipe). 990ul of amplification buffer was mixed with 10ul 0.15% H_2O_2 and 1ul tyramide. The tyramide included either DsRed flurorophore or AF488 (GFP). 30ul of the tyramide mixture was applied to each section and the slides were incubated in the dark, horizontally in falcon tubes at 46°C for 30minutes. The slides were then washed in 1x PBS in the dark for 10 minutes at room temperature, then rinsed in excess milliQ water followed by 95% ethanol. The slides were air dried in the dark prior to staining.

DAPI Staining

Following mono-FISH hybridization and washing or CARD-FISH amplification, the slides were stained with DAPI in mounting media. Enough mounting media was applied to cover the slide (~20ul per sample) and then covered with a covers slip. The slides were incubated at -20°C for 5 minutes and then were ready for imaging. Slides were stored at -20°C.

[Methodological notes: While fluorescently labeled microbes were consistently captured with both mono-FISH and CARD-FISH further optimization of the fixation and washing process will have to be done to capture an even section. Large pieces of fatty tissue often washed off following fixation and/or hybridization and may have carried microbial biomass with them. The sections imaged for this project were often patchy, and it was unclear if this was due to biology or the processing.]

Calcofluor Staining

For some sections prepared with the Eub1-3 CARD-FISH probe, calcofluor white M2R (Sigma Aldrich) was used to stain fungi. Calcofluor stains chitin and can be viewed with a fluorescence microscope using the UV (DAPI) filter. Calcofluor was dissolved in PBS to 0.1mg/ml concentration. 10ul was applied to each section and then the slides were incubated for 10 minutes in the dark at room temperature before being rinsed in excess 1x PBS. PBS was then used to prepare wet mounts.

Microscopy

Samples were imaged using a Zeiss Axio Scope.A1 with fluorescence filters and a Zeiss LM2780 point scanning confocal microscope with fluorescence capabilities and an argon laser. For confocal microscopy, z-stacks were conducted with the smallest step size possible (0.31um for 40x and 0.18um for 100x) for up to 40um of sample as determined by the highest and lowest plane where cells were in focus. The lasers were optimized to reduce oversaturation. For the images included here, the averaging was set to 4 and the speed to 7-9 depending on the depth of the z-stack.

Counting

Cells were counted using an ocular grid on the fluorescence microscope. The grid was 250um by 250um at 40x magnification and 100um by 100um at 100x magnification. At least 20 grids were counted for each measurement.

Statistics

Depth of oxygen depletion and fungal abundance were analyzed using Kruskal-Wallis one way ANOVA in R (R Core Team 2015).

Results

Microelectrode Profiles

Steep oxygen clines were observed in all of the three cheeses (Figure 1). The curved nature of this cline indicates that the reduction was due to biological activity and not just diffusion (W. Ziebis *pers. comm.*). The average depth at which oxygen initially reaches <1.5um did not differ significantly between cheese types (Figure 2; $p>0.05$). The average value was 300um ±0 for the Moses Sleeper cheese, 500um ±297 for Blue, and 316um ±98 for Willoughby. The lowest depth at which oxygen <1.5um was observed was 300um for the Moses Sleeper cheese, 200um for Blue, and 200um for Willoughby. The greatest depth at which oxygen >1.5um was observed was 2000um for the Moses Sleeper cheese, 1200um for Blue, and 375um for Willoughby. The unusually high value observed for the Moses Sleeper was driven by air pockets observed inside the curd of the cheese (Figure S.1), which are introduced during the mechanical compression of the curds (R. Dutton pers. comm.).

pH did not systematically vary in any of the cheese, but did differ between cheese types. Willoughby, the washed rind cheese, was the most basic, while Moses Sleeper and the Blue cheese were more neutral. These results were consistent with single point pH measurements from these cheeses (Wolfe *et al*. 2014). Temperature did not vary meaningfully over the time the profile was measured (data not shown) and instead reflected the conditions under which the cheeses were profiled (e.g., time spent on the bench).

Composition

Both bacteria and fungi were identified in all three cheese samples. It was possible to distinguish between some fungal taxa using morphology and the reference database (Wolfe *et al*. 2014) of taxa that were likely to be present in these samples. For example, in a single section of Moses Sleeper, we were able to identify filamentous fungi (likely *Penicillium spp.*; Figure 3A), rod-shaped unicellular fungi (likely *Galactomycetes spp.*; Figure 3B), and cocci unicellular fungi (likely Saccharomycetes; Figure 3C). Rod-shaped and cocci bacteria are also abundant in all of the sections imaged (e.g., Figure 4), but more precise taxonomic identification was not possible with the EUB338 I-III.

Colocalization between bacteria and fungi was extremely common and was observed in all cheese types and at all depths sampled. Some of the patterns observed included a few cells of bacteria associated with fungi (Figure 5A), bacterial aggregates surrounding single cells of fungi (Figure 5B), and biofilms of combined bacteria and fungi (Figure 5C). All of the fungal morphologies observed were seen with microbial associations. Notably, even in planes where bacterial-fungal colocalization was common, not all fungal cells were similarly associated with bacteria (Figure 6). Confocal microscopy provided a more detailed view of the colocalization across space (see Supplementary Video Files on course wiki) but did not produce qualitatively different results from single-plane fluorescence microscopy.

A difference in fungal abundance was observed between the top and bottom of the rind in Willoughby cheese (Figure 7; $p<0.0001$, $df=1$). Anecdotally, a difference in the Blue cheese was not observed, which makes intuitive sense because the cheese making process encourages fungal

growth into the curd. But, I was unable to quantify fungal abundance in the Blue or Moses Sleeper cheeses to an extent that statistical tests could be performed.

Discussion

As predicted, the abiotic environment varies within a cheese rind. A marked oxygen gradient is observed over the first few hundred microns and the shape of this gradient indicates that biological activity is responsible for the depletion of oxygen. In contrast, pH does not vary consistently. Therefore, it is to be expected that vertical variability in community composition primarily reflects differences in redox conditions, and in particular oxygen availability, although other variables not measured here may also play a role.

The potential for oxygen profiles to predict changes in community composition is well supported by data from environmental microbiological systems. Sediment, both freshwater and marine, communities also experience oxygen depletion with depth due to respiration, and this is reflected in the identity and function of the microbes present (e.g. Bertics and Ziebis 2009, He *et al*. 2015). Furthermore, oxygen gradients in the gut (from epithelial wall in to the lumen) are also predicted to shape the microbial communities (Albenberg *et al*. 2014).

The methods used here to profile the variation in composition of cheese through the rind did not identify major shifts along the vertical gradient. No major fungal morphotypes were absent consistently in any of the depths. And, while fungal abundance did decrease from the top of the rind to the bottom of the rind/curd interface in one of the cheeses surveyed, otherwise no consistent trends in fungal or microbial abundance were observed across the depths sampled.

However, both FISH and calcofluor staining were successful in capturing some of the *in situ* behavior of the microbial components of cheese rinds. Fungi and bacteria were found in close proximity, often physically touching, in all samples. Galactomycetes, or other rod-shaped single celled fungi, were particularly likely to be found colocalized with bacteria (e.g. Figure 5B, 5C). Previous coculture experiments have shown that Galactomycetes inhibits Staphylococcus, Arthrobacter, Brachybacterium, Brevibacterium, and Serratia while promoting the growth of Corynebacterium, Pseudomonas, Pseudoalteromonas, and Vibrio (Wolfe *et al*. 2014). Of the 6 fungi tested, it was the species that interacted with the most bacteria. This may be reflective of how often it is found around bacteria *in situ*.

The extensive amount of colocalized bacteria and fungi identifies an important area for future research. Physical proximity between bacteria and fungi was common—but not universal or consistent—in the cheeses sampled and indicates that direct or indirect interactions between bacteria and fungi is likely. With more targeted probes, it would be possible to identify the partners in these interactions and to define their specificity. With representative isolates, it would then be possible to begin to characterize these interactions *in vitro*.

Metagenomic profiling of the entire cheese rind (Wolfe *et al*. 2014) identified cytochrome oxidase B and C genes. Cytochrome oxidases B and C are both high-affinity oxidases, meaning they function under low-oxygen conditions (Morris and Schmidt 2013). In addition, many fermentation genes are present in the cheese rind indicating that microbial metabolism under microaerobic and anaerobic conditions is likely. Who is performing these metabolisms is unclear, however. Sequencing of sections from along the oxygen cline should help answer the outstanding question of if and how composition and function varies with depth and how this might be affected by oxygen availability.

Previous research into fully aged cheeses has treated the rind as a single functional unit (e.g. Feurer *et al*. 2004; Quigley *et al*. 2012; Wolfe *et al*. 2014). The results shown here

demonstrate that the environment varies significantly across the rind and that the composition can also vary. Further research expanding upon these techniques is needed to tie this environmental variation to compositional and functional variation. Microelectrode profiling and FISH will both be important tools in an effort to define the feedbacks between abiotic and biotic elements in this complex microbial system.

Acknowledgments
None of this work would've been possible without the tireless efforts of Jared Leadbetter and Dianne Newman to ensure this course could happen intellectually and financially and so I am deeply grateful to them first and foremost. I also received extensive help from Emil Ruff, Elise Cowley, Sebastian Kopf, Scott Dawson, Deb Hogan, and the staff at the microscopy facility on methods development and implementation. Rachel Dutton kindly provided cheese and her expertise on cheese to make this project happen. Finally, I would like to thank all of the other members of the course—student and faculty alike—for helping me talk through ideas and learn much about the microbial world.

References
Albenberg L, Esipova TV, Judge CP, Bittinger K, et al. 2014. Correlation between intraluminal oxygen gradient and radial partitioning of intestinal microbiota. *Gastroenterology* **147**:1055-1063.
Baschien C, Manz W, Neu T, Szewzyk U. 2001. Fluorescence in situ hybridization of freshwater fungi. *International Review of Hydrobiology* 86:371-381.
Bertics VJ, W Ziebis. 2009. Biodiviserstity of benthic microbial communities in bioturbated coastal sediments is controlled by geochemical microniches. *The ISME Journal* **3**:1269-1285.
Bonfante P, I Anca. 2009. Plants, mycorrhizal fungi, and bacteria: a network of interactions. *Annual Review of Microbiology* **63**:363-383
Cowley ES, Kopf SH, LaRiveriere A, Ziebis W, Newman DK. 2015. Pediatric Cystic Fibrosis Sputum Can Be Chemically Dynamic, Anoxic, and Extremely Reduced Due to Hydrogen Sulfide Formation. mBio 6: e00767-15.
de Boer W, Folman LB, Summerbell RC, Boddy L. 2005. Living in a fungal world: impact of fungi on soil bacterial niche development. *FEMS Microbiology Reviews* **29**:795-811.
Feurer C, Irlinger F, Spinnler HE, Glaser P, Vallaeys T. 2004. Assessment of the rind microbial diversity in a farmhouse-produced vs a pasteurized industrially produced soft red-smear cheese using both cultivation and rDNA-based methods. *Journal of Applied Microbiology* **97**:546-556.
He S, Malfatti SA, McFarland JW, Anderson FE, Pati A, et al. 2015. Patterns in wetland microbial community composition and functional gene repertoire associated with methane emissions. *mBio* **6**:e00066-15.
Morris RL, Schmidt TM. 2013. Shallow breathing: bacterial life at low O2. *Nature Reviews Microbiology* **11**:205-212.
Quigley L, O'Sullivan O, Beresford TP, Ross RP, Fitzgerald GF, Cotter PD. 2012. High-throughput sequencing for detection of subpopulations of bacteria not previously associated with artisanal cheeses. *Applied and Environmental Microbiology* **78**:5717-5723.
Revsbech NP, Sorensen J, Blackburn TH, Lomholt JP. 1980. Distribution of oxygen in marine sediments measured with microelectrodes. *Limnology and Oceanography* **25**:403-411.
Wargo MJ, DA Hogan. 2006. Fungal-bacterial interactions: a mixed bag of mingling microbes. *Current opinion microbiology* **9**:359-364.

Wolfe BE, Button JE, Santarelli M, and Dutton R. 2014. Cheese rind communities provide tractable systems for *in situ* and *in vitro* studies of microbial diversity. *Cell* **158**: 422–433.

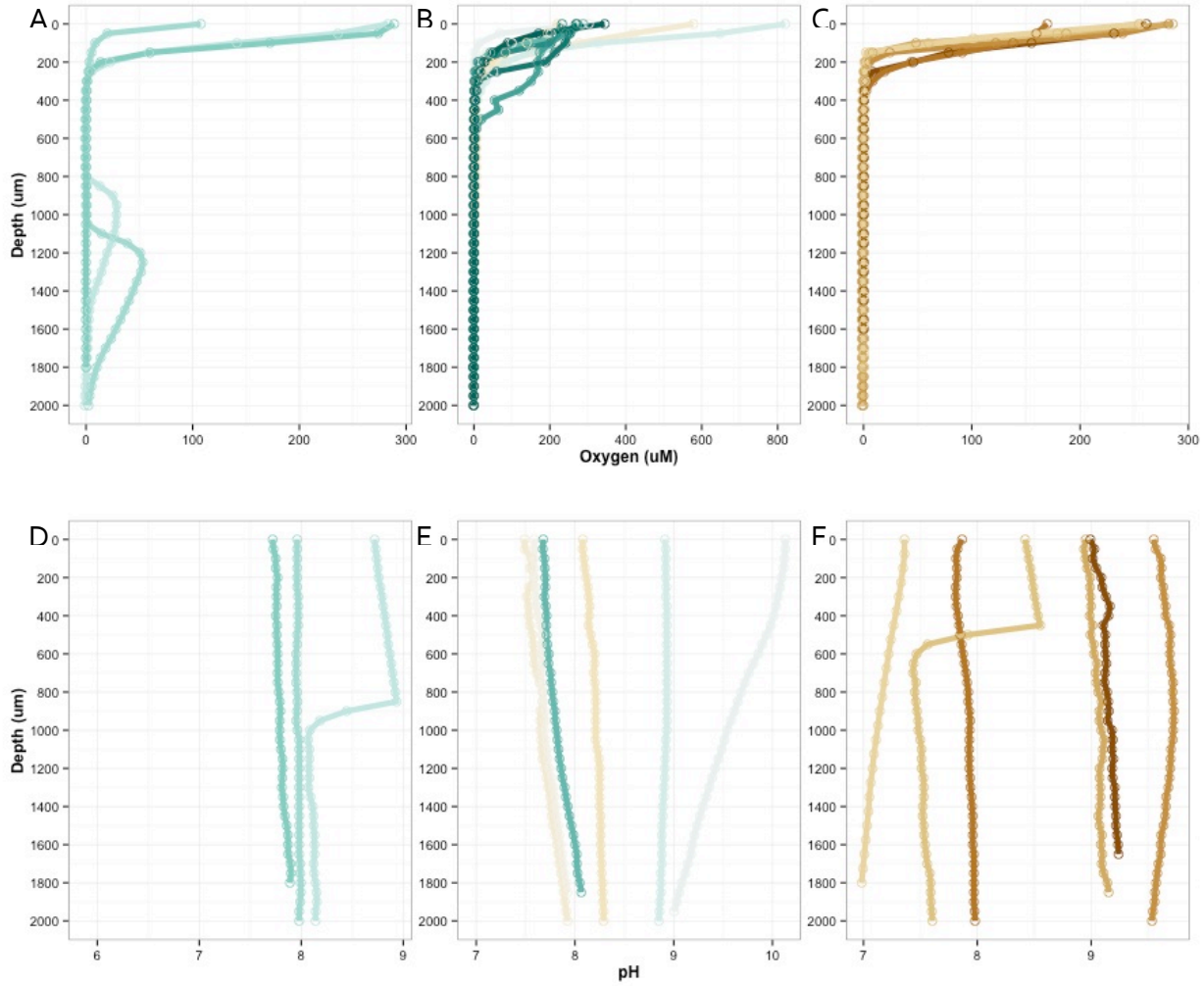

Figure 1 Microsensor profiles of O2 and pH from the surface of the rind to 2mm below the rind. Oxygen shows reproducible gradient with curve characteristic of biological consumption in all three cheeses (A-C). pH does not vary consistently within cheeses but does differ between cheeses (D-F).

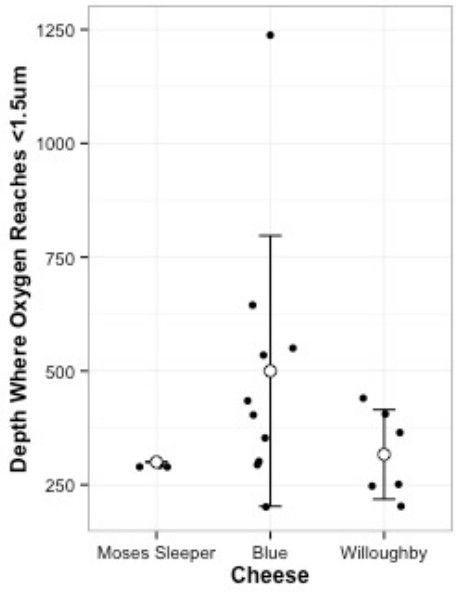

Figure 2 Average depth at which oxygen reaches less than 1.5um concentration does not differ significantly between cheese types. White points indicate average for cheese type and black points are actual measurements. Error bars indicate standard deviation.

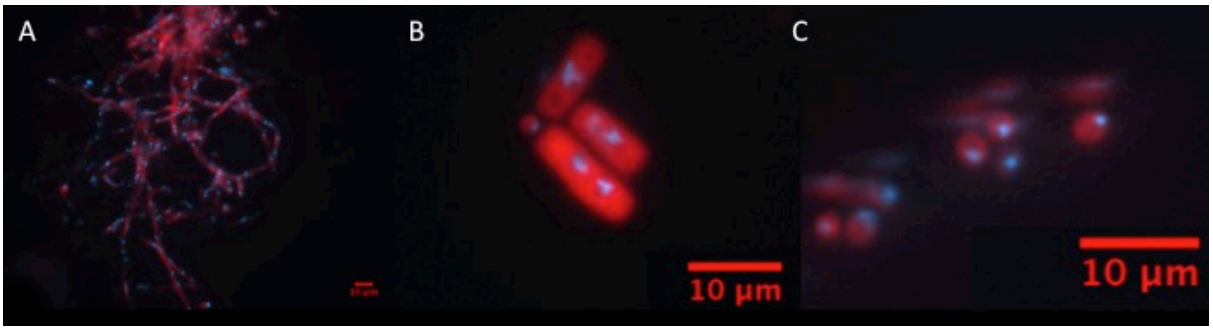

Figure 3 Representative fungal images from Moses Sleeper section from 0um depth. Fungi are stained with EUK516 mono-FISH probe. Bacteria and fungal nuclei are stained with DAPI. All scale bars are 10um.

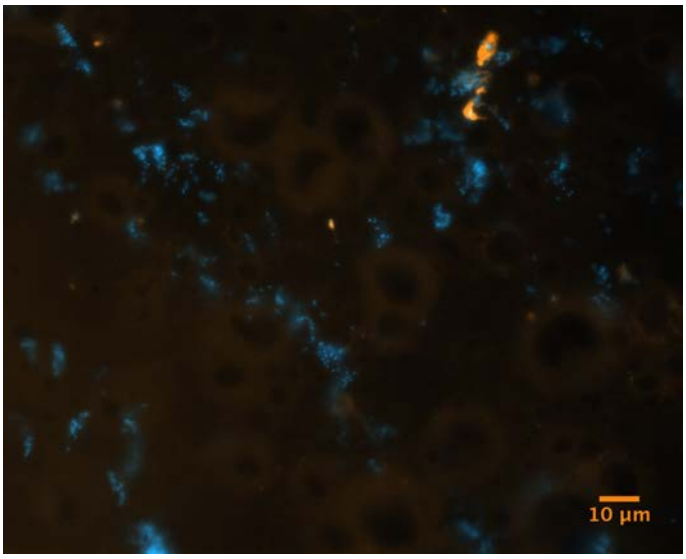

Figure 4 Representative bacterial image from Willoughby section from 1000um depth. Bacteria and fungal nuclei are stained with DAPI and fungi with EUK516 CARD-FISH probe.

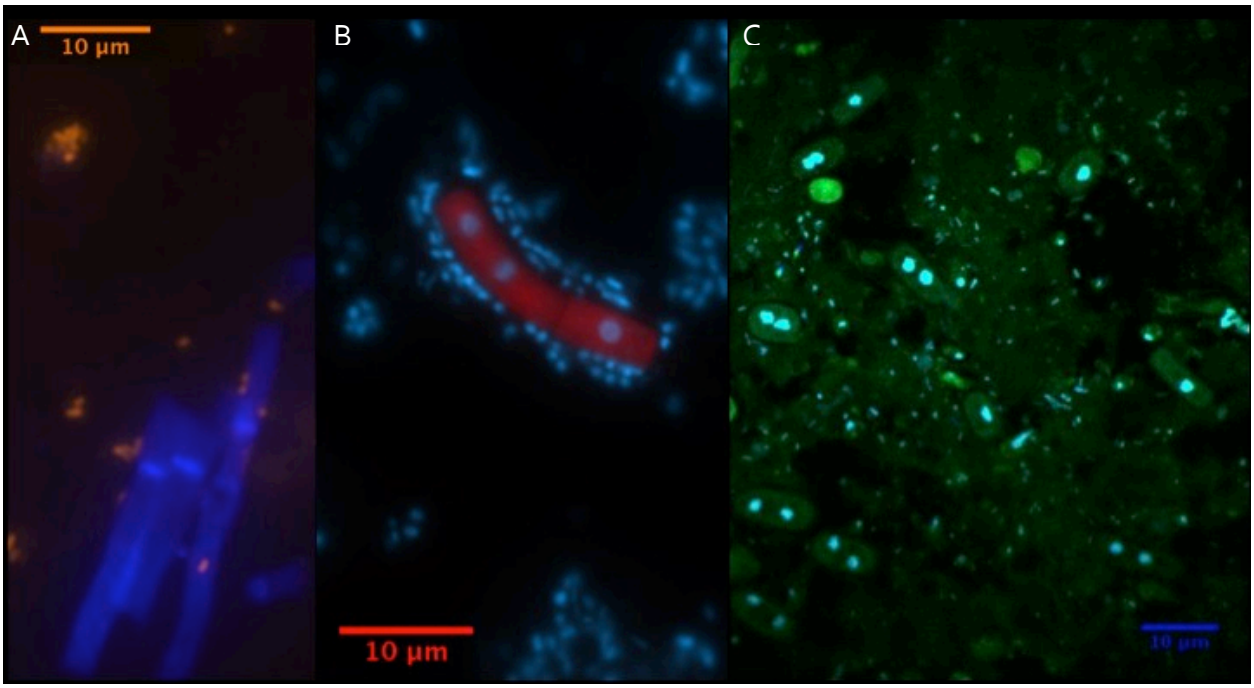

Figure 5 Representative colocalization images. A. Blue 750um Calcofluor (blue) and EUB338I-III CARD-FISH (orange); B. Willoughby 0um EUK516 mono-FISH (red) and DAPI (blue); C. Willoughby 0um EUK516 CARD-FISH (green) and DAPI (blue). All scale bars are 10um.

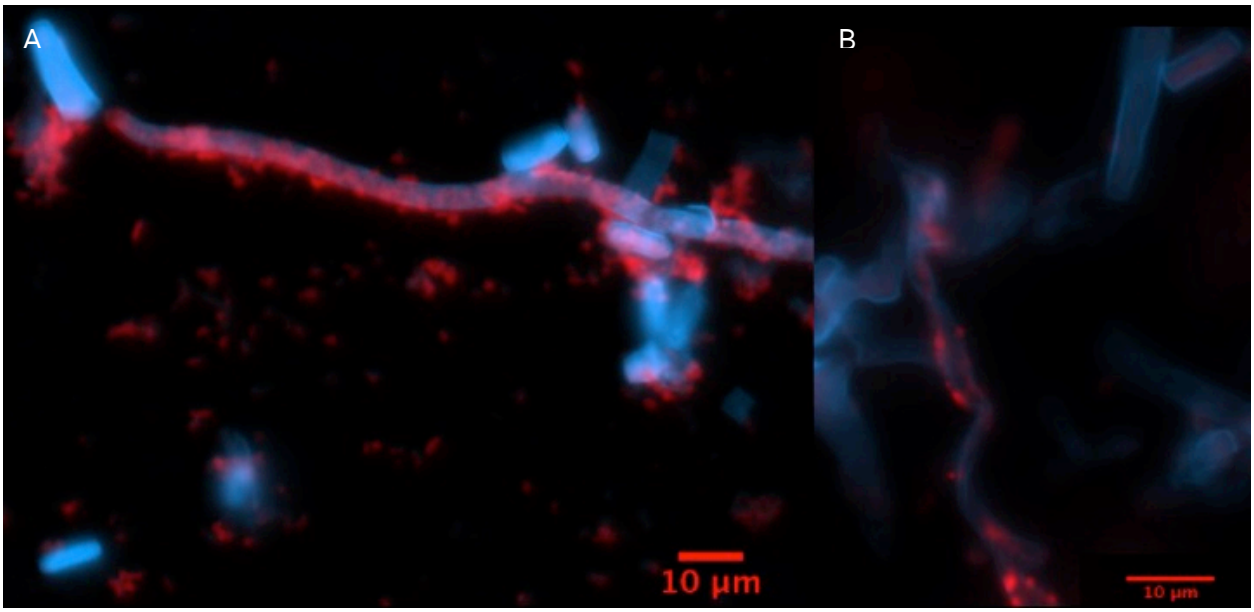

Figure 6 Representative images of specific colocalization. A. Willoughby 500um with Calcofluor chitin stain (blue) and EUB338I-III CARD-FISH (red); B. Moses Sleeper 350um Calcofluor chitin stain (blue) and EUB338I-III CARD-FISH (red). All scale bars are 10um.

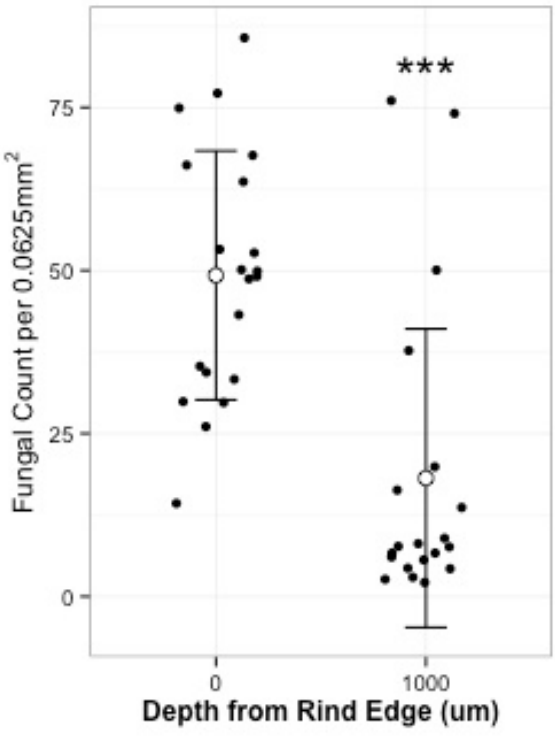

Figure 7 Fungal abundance at 0um depth (N=20) is significantly greater ($p<0.0001$) than at 1000um (N=20) in Willoughby cheese. White points indicate average for depth and black points are actual measurements. Error bars indicate standard deviation.

Appendix

Lysozyme solution for 50mL
100mg lysozyme
5ml 0.5M EDTA
5ml 1M Tris, pH8
40ml milliQ water

Chitinase solution for 50mL
50mg of chitinase
50ml 50mM potassium phosphate, pH 6.0 (0.32g KH_2PO_4 and 0.0326g K_2HPO_4 per 50ml milliQ water).

Washing buffer for 50ml
0.5ml 0.5 M EDTA, pH 8.0
1.0ml 1 M Tris HCl, pH 8.0
700ul NaCl
47.775ml milliQ water
25ul SDS (20% w/v; added last)

CARD hybridization buffer for 20mL, 35% formamide concentration
3.6mL 5M NaCl
0.4mL 1M Tris, pH 8.0
20uL SDS (20%w/v)
2.0 mL blocking solution
7ml formamide
7ml sterile milliQ water
2.0 g of dextran sulfate
Heated in 60C water bath until dextran sulfate dissolved completely. 1ml aliquots were stored at -20C.

CARD amplification buffer for 40mL
4.0mL of 10x PBS, pH 7.4
0.4mL blocking solution
16mL 5M NaCl
19.6mL milliQ water
4g dextran sulfate.
Heated in 60C water bath until dextran sulfate dissolved completely. 1ml aliquots were stored at -20C.

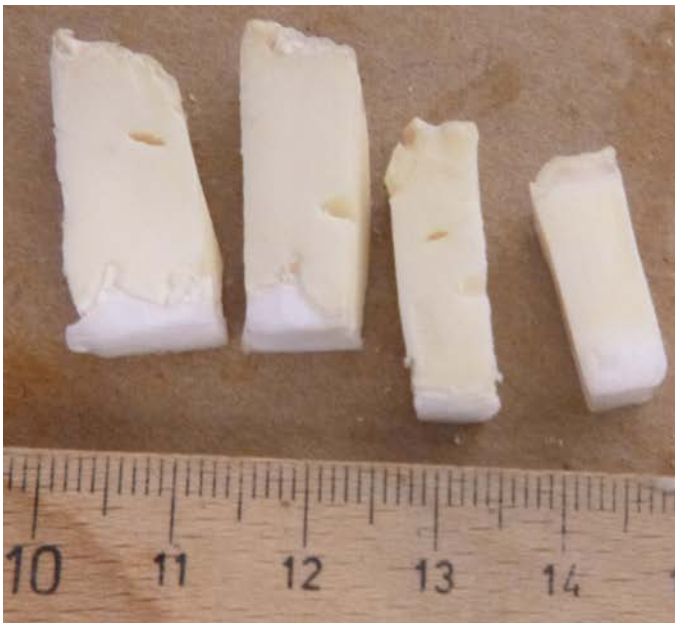

Figure S. 1 Air pockets in Moses Sleeper. Rind is on the top of the image. White material at the bottom of the cheese is frozen OCT.